

RSC Advances



This is an *Accepted Manuscript*, which has been through the Royal Society of Chemistry peer review process and has been accepted for publication.

Accepted Manuscripts are published online shortly after acceptance, before technical editing, formatting and proof reading. Using this free service, authors can make their results available to the community, in citable form, before we publish the edited article. This *Accepted Manuscript* will be replaced by the edited, formatted and paginated article as soon as this is available.

You can find more information about *Accepted Manuscripts* in the [Information for Authors](#).

Please note that technical editing may introduce minor changes to the text and/or graphics, which may alter content. The journal's standard [Terms & Conditions](#) and the [Ethical guidelines](#) still apply. In no event shall the Royal Society of Chemistry be held responsible for any errors or omissions in this *Accepted Manuscript* or any consequences arising from the use of any information it contains.

Fine tuning of band-gap of graphene by atomic and molecular doping: A density functional theory study

Akhtar Hussain^{a*}, Saif Ullah^b, M. Arshad Farhan^c

^aTPD, Pakistan Institute of Nuclear Science and Technology (PINSTECH), P. O. Nilore, Islamabad, Pakistan.

*E-mail: ahmohal@yahoo.com

^bDNE, Pakistan Institute of Engineering and Applied Sciences, P. O. Nilore, Islamabad, Pakistan

^cEMMG, Physics Division, PINSTECH, P. O. Nilore, Islamabad, Pakistan.

First-principles density functional theory (DFT) based calculations were carried out to investigate the structural and electronic properties of beryllium (Be) and nitrogen (N) co-doped and BeN/BeO molecular doped graphene systems. The basic focus was on how the band-gap can be fine-tuned with concentration and replacement/site(s) variations. It was interesting to note that with this hetero combination of electrons (N) and holes (Be), doped graphene systems increase in concentration do not always lead to a higher band-gap. The insertion of holes and electrons at hetero sites simultaneously, leads to increase the energy-gap. However, if the replacement combination of sites comprises of same rectangular or hexagonal ones, then band-gap may decrease with increasing impurity concentration. Additionally, the insertion of BeO molecule(s) is also position dependent and band-gap enhancement is not always proportional to the density of doped BeO molecules. Finally, our results suggest that having control on the dopant position, a very fine tuning of the band-gap is possible which make graphene a favorable material for its utilization in diverse electronic device applications.

1 Introduction

Graphene is a one-atom-thick sp^2 -hybridized monolayer of carbon atoms with a two-dimensional (2D) honeycomb lattice structure. It forms the building block of all other graphitic materials, such as 0D fullerenes (Bucky ball), 1D nanotubes and 3D graphite.¹⁻⁴ Since its discovery in 2004¹, the famous nanomaterial, attracted the attention of researcher working in various fields of science because of its fascinating properties and potential applications in electronic⁵⁻⁸, spintronic⁹⁻¹² physical, electrical, and optical properties^{1;9;13;14} with tremendous charge carrier mobility of about $106 \text{ cm}^2 \text{ Vs}^{-1}$, which is 2–3 times greater than conventional semiconductors.¹⁵The 2D material graphene was synthesized using

mechanical exfoliation technique discovered by Geim and Novoselov who were awarded the Nobel Prize in Physics in 2010. Its honeycomb structure is build such that in every graphene unit cell there are two nonequivalent carbon (C) atoms, which can be considered as two interweaving triangular sub-lattices, as shown in Fig. 2(a). Each carbon atom, establishes three strong σ bonds with the other three surrounding carbon atoms in addition to three π bonds.

Despite having extremely useful properties associated with graphene, a major issue limiting its use in semiconductor electronic devices is its zero band-gap. According to tight-binding calculations carried out by Nato et al⁴, the valence and conduction bands touch at the Brillouin zone.¹⁶ This problem of band-gap-less dispersion in graphene hinders electronic devices such as field-effect transistors (FETs) fabrications. To make it useful for realistic applications, it is desirable to modify the band structure of graphene for switch off/on devices¹⁷ as per requirement. This makes, the band-gap engineering¹⁸ of graphene an essential and important topic with regard to applications. To cope with the band-gap issue, certain techniques are being used including designing superstructures of graphene-like nanoribbons,^{19;20} quantum dots,^{21;22} and nanomeshes.²³ Doping (to introduce impurities such as adsorbing or substitutional atoms) is another efficient way to tailor the electronic, chemical and magnetic properties of materials. The doping of graphene came into sight just after the isolation of graphene in 2004⁹ and is now turning into a sizzling area. Replacement of C-atoms with suitable impurity atoms open up an energy gap between the valence and conduction band. The doping in graphene can be classified into electrical and chemical doping. The doping is referred to as the chemical one when the changes in the graphene lattice structures result via chemical routes, such as substitutional doping with heteroatoms,²⁴ or molecules.²⁵ The goals achieved from such modifications strongly depend on the type of dopants, concentrations and their location within the graphene systems.²⁶

The chosen sites of graphene for replacement with the foreign impurity atoms are of critical importance where Fermi level depends upon the concentration of doped holes and electrons. The Fermi level of graphene doped system may either lower or rise from zero adjusted level depending upon the dopant type and replacement site. The electron deficient foreign doped atoms (relative to that of C-atoms) such as Al, B, Be, NO₂, H₂O, and F4-TCNQ cause Fermi-level to shift downward thereby exhibiting p-type doping. On the other hand electronically rich substituted atoms such as N, and alkali metals enhance the Fermi level exhibiting n-type doping²⁷⁻³³. These dopants significantly alter the electronic structure of graphene and induce a band-gap. Substitutional doping is most suitable in the case where the closest neighbor of

carbon like boron (B), beryllium (Be), nitrogen (N) and oxygen (O) are selected to replace C-atoms.^{26;34-36;36-39} Additionally, dopants vary the chemical reactivity of graphene, which in turn can be used as bio-sensors towards many atoms, molecules and gases^{40;40;41}.

Beryllium (Be) is lighter atom compared to C having 2 valence electrons with an electronic configuration $1s^2 2s^2 2p^0$. Be can be integrated in graphene. At high melting temperatures of about 1500 K, Be atoms can be arranged to form an hexagonal close packed (hcp) crystal structure. The synthesis of beryllium carbide (Be_2C), which is a hard material, can be achieved by heating Be and C at about 1173.15 K. DFT calculations were carried out by Ferro et al.⁴² to investigate the absorption and diffusion of Be in graphite and the formation of Be_2C . The authors found that the high absorption of Be in graphite can lead to the creation of Be_2C . Be can also be doped in graphene by using chemical vapor deposition (CVD) techniques. The doping of light atoms to graphene has induced band-gap in graphene in previous investigations⁴³. Electron deficient B and electron rich N (relative to C) have been substituted in graphene and, the maximum band-gaps of 0.72 eV were observed at a 12% dopants concentration as per reported GGA-PBE calculation of DFT.⁴⁴ In our recent publication Be has been found to be more efficient than B or N in inducing the band-gap in graphene. It was concluded that both the concentration of the impurity atom(s) and location of graphene C-atom(s) to be replaced were very important.²⁶

In our recent past study a band-gap of graphene has been engineered by doping of Be and different combinations of Be with B. The maximum value of energy gap of 1.44 eV was computed in a particular Be doped graphene system. In the current study, an attempt has been made to open up an energy gap by substitutional doping with beryllium and co-doping of Be with N in addition to planer mode doping of BeO molecule in graphene sheet. The doping concentration and effective doping positions have been investigated systematically. The paper is arranged in a way that firstly, the structural properties and electronic band structures of Be and N co-doped graphene with varying site and concentration are reported, secondly planer substitution of BeO molecule with variant concentration and position is discussed.

2 Details of computation

First-principles calculations were performed with the Vienna ab initio simulation package (VASP) based on density functional theory (DFT).^{45;46} The electron-ion interaction was described by the projected augmented wave (PAW)⁴⁷ method and the Perdew, Burke, and Ernzerhof (PBE)⁴⁸ version of the generalized gradient approximation (GGA) was adopted for exchange and correlation parts of the electron-electron interactions. The plane-

wave cutoff energy was set to 450 eV. A slab model consisting of a 4 x 4 graphene supercell (32 atoms) was selected. Periodic boundary conditions were applied in all directions. In order to avoid artificial interlayer interactions, the vertical separation between the two sheets was fixed $> 14 \text{ \AA}$. We have doped equal amount of Be, N and BeO concentration thus generating equal number of C–Be, C–N and C–O bonds. Monkhorst–Pack grids are used to sample the Brillouin zone with 9 x 9 x 1 Gamma-centered k mesh.⁴⁹ For the density of states (DOS) a denser K-point grid of 16 x 16 x 1 was used. A first-order Methfessel–Paxton smearing-function with a width $\leq 0.1 \text{ eV}$ was used to account for fractional occupancies.⁵⁰ Energy minimizations of the structures were performed until the total Hellmann–Feynman forces were smaller than 0.01 eV/\AA .⁵¹ All the atoms in the systems were relaxed during geometry optimization process. With the aim to give a numerical account of the strength of the doped systems, cohesive energy was calculated using the formula:

$$E_{\text{coh}} = [E_{\text{tot}} - \sum_i n_i E_i] / n \quad (i = \text{C, Be, N, O}),$$

where E_{coh} is the cohesive energy per atom of Be, N and O doped configuration. E_{tot} and E_i represent total energies of a structure and of individual elements present within the same supercell, respectively. Finally, n_i is the number of i th species present in the configuration, while n being the total number of atoms. Initially spin polarized calculations were performed to check the stability issues. It was found that spin-polarized and non-spin polarized calculations gave the same results as graphene is non-magnetic material. Thus, rest of the calculations performed were restricted to non-spin polarized for computational simplicity.

3 Results and Discussion

We replaced C atoms with 1Be, 1N; 2Be, 2N; 2Be, 3N atoms and 1BeO, 2BeO and 3BeO molecules at variant positions as it is interesting to dope graphene with dual hetero-species^{32;33}. We obtained different values of band-gaps depending upon the concentration and dopant site. The results obtained are discussed below systematically.

3.1 Atomic doping

3.1.1 1Be, 1N in one hexagon

As preliminary step, we calculated the effect of doping of 1Be (beryllium) and 1N (nitrogen) atoms in a single hexagon of 4x4 unit cell of graphene to examine the stability and band gap by varying the position of the dopants at ortho, meta and para positions similar to

those found in a benzene ring. It was found that when Be & N are replaced with the two consecutive /adjacent C atoms (3,4 positions), the system remains the most stable relative to all other configurations as shown in Table 1; thus showing the priority of BeN (beryllium nitride) formation. The least stable arrangement is found for 2,6 position of Be and N respectively, which is energetically 2.47 eV less stable relative to the 3,4 configuration (Be-N adjacent) as presented in the table 1. Stability of all other patterns of Be and N atom doping within a single hexagon of graphene sheet remains in between these two limits. The relative stability of the structure remains unchanged with or without spin polarization. It is worth noting that except the 3,4 configuration described above, there does not exist any direct σ -bond between Be and N atoms. Therefore, addition of spin polarization might not affect the band gap substantially.

The band structure was computed for each case. The band-gap remains slightly above the Fermi-level and amounts to 0.24 eV except for the case when Be and N are accommodated at 1,4 locations of a hexagon where band-gap substantially enhances to 0.50 eV. In this case both dopants occupy the positions which are maximally distant in a hexagon. The nature of the band gap is direct one for all the above mentioned cases. The previously mentioned calculations refers to in-plane substitution where N substitutes an sp^2 -hybridized C atom. The next logical step was to check the functionality of N atom on top of graphene where it is sp^3 -hybridized. The most stable configuration results when N is adsorbed at the top of Be atom. During the optimization process, N moves downward to the level of graphene resulting in downward push of the Be atom from the graphene plane distorting the nearby atoms' equilibrium structure as well as depicted in Figure 1(a, b). The Be-N bond length was measured to be 1.75 Å. The N was placed at bridge and hollow positions also, but during optimization procedure the final configuration becomes as mentioned above. The second configuration was achieved by placing N at C atom opposite to the Be atom in a hexagon which finally converges by bridging between two C-atoms as shown in Figure 1(d, e). The structure of the system results in a significant distortion in addition to notable (4.41 eV) desalination relative to previous case (see Table 1).

The band structure calculations show a band-gap of 0.88 eV as shown in Figure 1(c) in top adsorption case. This value of energy-gap is significantly higher relative to in-plane substitution. In case of N bridged bonded, the band-gap rises above to the Fermi level. The amount of resulting direct gap is found to be 0.38eV as shown in Figure 1(f). It is worth concluding here that the substituted N replaces the in-plane C-atom, therefore, the functionality of doped nitrogen is always three making it more similar to sp^2 hybridized

pyridinic N. However, calculations for doping Be-N system by replacing one single carbon atom and adsorbing N-atom results in displacing the N to either on a bridge position or distort the structure to make Be-N molecule as shown in Figure 1. In these cases, the functionality of these configurations is changed to quaternary from pyridinic type.

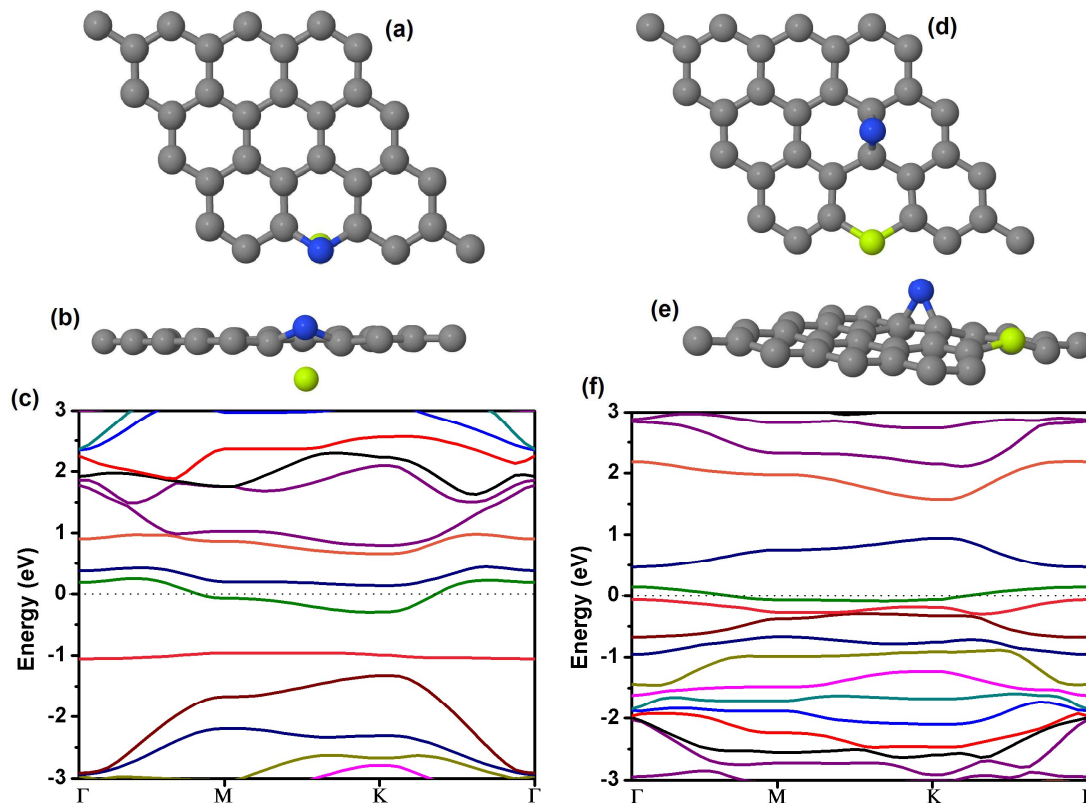


Figure 1. The optimized geometry of graphene sheet co-doped with one Be (green sphere) and one N atom (blue sphere) is shown in part (a) in a non-planar mode. The side view is shown in part (b). The parts (d) and (e) depict when N-atom adsorbed on bridge position of the adjacent hexagon of graphene to that where Be-atom is doped planerly. The band structures of these optimized geometries are depicted in (c) and (f).

Table 1: shows energetically destabilization on Be and N doping in a single hexagon (Sr. No. 1-6) and in the different hexagons of the grapheme structure (Sr. No. 7-18). The energy of pure grapheme has been assumed as 0.0 eV and the relative disability with respect this structure due to foreign dopants replacement has been given for each case. It should be noted that systems at Sr. No. 19 and 20 are comprised of 33 atoms. The positions of Be and N have been varied at para, meta and ortho positions. Entries in brackets show the

destabilization in a system when compared to the most stable system at Sr. No. 3 and for N-functionality at Sr. No. 19.

Sr. No.	System	Optimized doped system	System description/ configuration	Nature of calculations	
				Non-spin polarized	Spin polarized
	Graphene		C-32	0.0	0.0
1	Be-N doped		3,4 position of same hexagon	+9.47	+9.47
2	Be-N		1,5 position of same hexagon	+11.91 (2.44)	+11.91
3	Be-N		3,5 position of same hexagon	+11.74 (2.27)	+11.74
4	Be-N		2,6 position of same hexagon	+11.94 (2.47)	+11.94
5	Be-N		1,3 position of same hexagon	+11.72 (2.25)	+11.72
6	Be-N		1,4 position of same hexagon	+12.07 (2.60)	+12.07
7	Be-N		Pattern I (B & N at different hexagons)	+12.13	
8	Be-N		Pattern II (dopants at different hexagons in all the following cases)	+12.20	
9	2Be2N		Pattern I	+23.99	
10			Pattern II	+23.69	
11	2Be3N		Pattern I	+24.89	
12			Pattern II	+24.49	
13			Pattern III	+24.81	
14	1BeO			+12.09	
15	2BeO		Pattern I	+24.27	

16	2BeO		Pattern II	+24.60	
17	3BeO		Pattern I	+36.64	
18	3BeO		Pattern II	+36.56	
19	Be-N		N-functionality (top)	+2.42	
20	Be-N		N-functionality (bridge)	+6.83 (+4.41)	

3.1.2 1Be, 1N (pattern I)

In the second step we doped one atom each of Be and N in graphene (making impurity concentration of 6.25 %). In our recent investigations,²⁶ we impured the graphene with electron deficient (relative to C) Be and B atoms. This study relates the combination of both the electron rich N and electron deficient Be used as dopant in graphene. Initially, both the impurity atoms are assigned at the same sub-lattice positions. The details regarding the different types of sites available in graphene are discussed in details in reference.²⁶ The structure undergoes geometrical changes as a result of optimization as per prescribed criteria. The bonds around Be atom are elongated either to 1.55 or 1.56 Å similar to structural changes around single Be atom doping in graphene sheet.²⁶ The N-C nearest neighboring bonds are either found to be 1.39 or 1.40 Å, which is also in a good agreement to prior DFT (GGA) studies.^{29;43;44;44} Thus, reduction in C-C bonds occurred in the vicinity of both the Be as well as N atoms. The bonds variations can be seen in Figure 2(a). The N-C bonds lengths are close to C-C bonds (1.42 Å in pristine graphene), because the covalent radius of N (71 pm) is closer to that of C (75 pm) relative to Be.

The cohesive energy of the system is calculated to be – 8.73 eV/atom, slightly greater than the co-doping of single Be with B (-8.72 eV/atom) in graphene sheet.²⁶ It is due to nearly the same size of N as compared to B. The greater electro-negativity of N (than Be as well as C-atom) results in the charge transfer from Be and C to N atom. Be atom transfer all its 2e (valence) charge, which is also in good agreement with our previous calculations,²⁶ while C atoms transfer 0.74e (average 0.024e per C atom) charge to N atom as shown by Bader charge analysis. N atom gained 2.74e charge which can be seen in iso-surface plot of charge density (see Figure 2 (b)).

The calculated band structure of this geometry is shown in Figure 2(c). As the Be is electron deficient and N is electron rich compared to C atom, so we are doping graphene sheet with holes (Be) and electrons (N) simultaneously on the same sub-lattice sites.

Additionally, Be has two electrons less and N has one more electron than C atom thus making the overall system electron deficient relative to the original graphene. Consequently, the Fermi level is shifted downward by 0.36 eV below the Dirac point. Thus our doping can be regarded as p-type. This shift in Fermi level is very minute than the co-doping of Be with B (1.13 eV)²⁶ in graphene sheet. The reason is, Be and B both are referred to as hole doping in graphene, while in this case, impurity (Be) acts as hole while other (N) serves as electron doping. With this combination and concentration of the hetero doped atoms, a band-gap opening of 0.30 eV was observed at Dirac point. This band-gap is produced due to the unbalancing of symmetry of two sub-lattices graphene. The value of this band-gap is small compared to single Be with B co-doping (0.49 eV).²⁶ The linear dispersion around Dirac point is not much affected by impurity atoms and hence, preserving its mobility up to a large extent, which can be used in ultrafast nano-electronic devices.

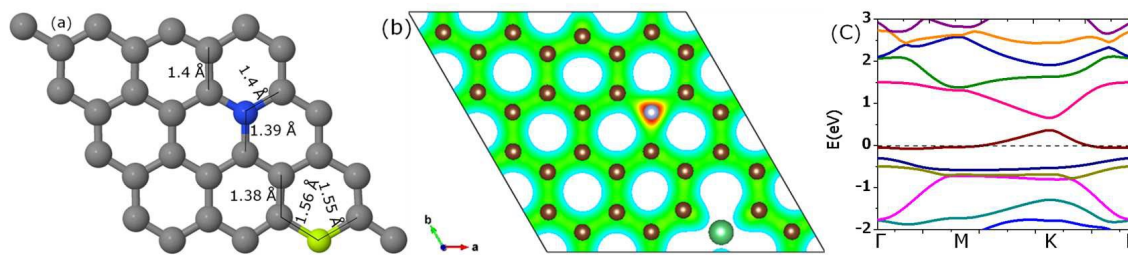


Figure 2: The optimized geometry of graphene sheet (pattern I) co-doped with one Be (green sphere) and one N atom (blue sphere) is shown in part (a). Iso-surface plot of charge density can be seen in part (b). The band structure of this optimized geometry is depicted in (c).

3.1.3 1Be, 1N (pattern-II)

The same impurity atoms as in above case are doped in graphene sheet at different positions. Now Be and N are injected in graphene sheet at different sub-lattice sites. The geometric/structural changes around Be-atom are found to be the same as in above case. The C-N bonds in the proximity of N atom range from 1.39 to 1.40 Å in length. The C-C bonds disturbance around the locality of Be and N are also similar as found for the system described in previous section (see Figure 3 (a)). The calculated cohesive energy is -8.73 eV/atom, agreeing well with the pattern-I model system described above showing the same structural stability of both the models. Likewise, Be atom has rendered all its 2e (valence) charge. The transfer of charge (0.65e) from C-atoms also occurred. The charge transferred per C-atom to nitrogen impurity is found to be 0.02e. Resultantly, N specie gained a charge of 2.65e. This

value is slightly lower than the value obtained for the system in pattern I because electron rich and electron deficient species sit on different sub-lattices. This local charge density gained around the N atom can be seen in the form of denser spots in iso-surface plot of charge density. The Fermi level downward shift below the Dirac point is 0.43 eV, which is higher than found in the pattern I case (0.36 eV). On the other hand band-gap opening of 0.62 eV is found, which is significantly higher than the band-gap value system in pattern I (0.30 eV). This value is higher than compared to the system co-doped with one Be and one B species (0.49 eV).²⁶

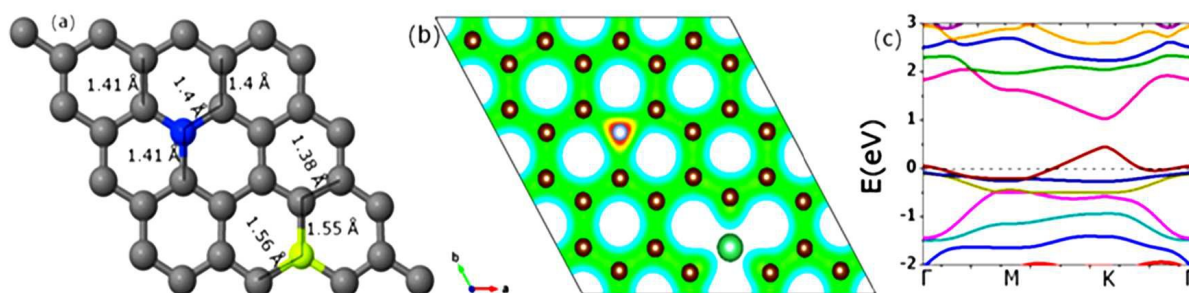


Figure 3: The optimized geometry of graphene sheet (pattern-II) co-doped with one Be (green sphere) and one N atom (blue sphere) is shown in part (a). Charge density plot can be seen in part (b). The band structure of this optimized geometry is depicted in (c).

In both the cases, same types of impurity atoms with the same concentration are doped at different sites, which result into different value of band-gaps. Unlike to our prior study of co-doping of Be with B²⁶, in this study we achieved a higher value of band-gap when dopants are integrated at different sub-lattices positions. This is due to the fact that Be acts as hole dopant while N acts as electron dopant in graphene sheet. So, on one sub-lattice site we are injecting holes and at the same time, on the other sub-lattice site electrons are infused. This causes to imbalance the two graphene sub-lattice symmetry significantly, resulting into band-gap opening of higher value. Isomers formed by choosing different doping sites differ significantly in relative stability and band gap introduced and these aspects, to a great extent, depend upon position of Be and N atoms in the hetero-structure agreeing well with a previous DFT study.⁴³

3.1.4 Two Be, two N (pattern-I)

In the next step, we increased the dopant concentrations to 2Be, 2N and 2Be, 3N at the same as well as the different sub-lattice sites. We found that by increasing the dopant concentration, the value of band gap decreases but the direct band-gap changes into indirect

one. Moreover, the linear dispersion at Dirac point is completely destroyed. The results are summarized in Table 2.

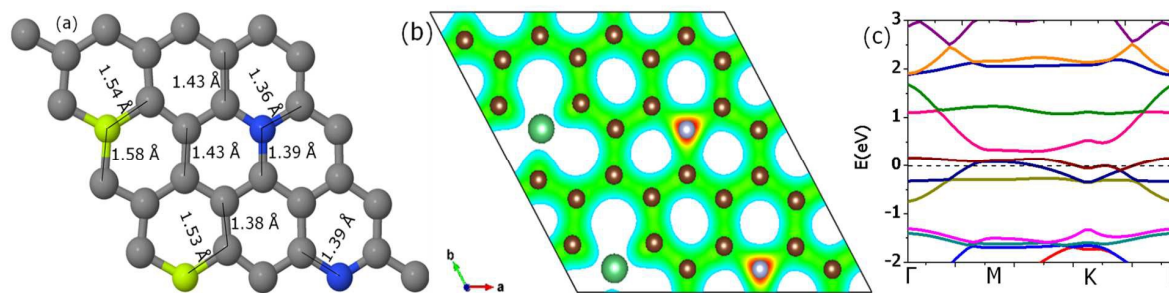


Figure 4: The optimized geometry of graphene sheet co-doped with 2 Be and 2 N atom (pattern-I) is shown in part (a). Charge density plot can be seen in part (b). The band structure of this optimized geometry is depicted in (c).

Four C-atoms are replaced by two Be and two N atoms making the concentration 12.5 % of the impurity atoms in graphene sheet. All impurity atoms are embedded at same sub-lattice positions. The bonds in the locality of Be atoms are extended having range from 1.53 to 1.58 Å while the reduction in the N-C bonds is as low as 1.36 Å. These bond length variations affect the neighbor C-C bonds of Be and N atoms (see Fig. 4). Cohesive energy was found to be -8.27 eV/atom, which is higher than two Be with two B doped graphene (-8.19 eV/atom). Thus N makes slightly better chemistry with C relative to B. However, the cohesive energy is sufficiently decreased by increasing the dopants from two (-8.73 eV/atom) to four atoms resulting in relatively lower stability of the structure. We found that Be atoms transferred all their valence charge ($2e$), while C atoms shifted $1.62e$ to N atoms. The average charge transferred per C-atom is $0.06e$. The charge gain per N impurity is $2.81e$. This charge accumulation around N species can also be seen in the iso-surface plot of charge density in Figure 4(b). The observed band-gap is found in somewhere middle of K and M line having a value of 0.23 eV, much lower than the value obtained for the system described in pattern II of 6.25% concentration. The linear dispersion near Dirac point is completely destroyed, resulting into the degradation of the mobility. It may be deduced that we are adding holes (Be) and electrons (N) at same sub-lattice positions, resulting in lesser symmetry breaking due to which small value of band-gap is induced.

3.1.5 Two Be, two N (pattern II)

The same concentration of impurity atoms as in above case are integrated in graphene sheet in pattern-II. However, the sub-lattice positions of Be atoms were different than N-atoms. The Be-C neighboring bonds are elongated either to 1.53 or 1.58 Å. The N-C bonds are shortened up to 1.38 Å. The next bordering C-C bond length in the proximity of Be as well as N are found to be changed as depicted in Figure 5. The calculated cohesive energy was -8.28 eV/atom agreeing well with the above system (-8.27 eV/atom). The transfer of valence charge i.e., $2e$ from Be atoms and $1.42e$ from C atoms to N impurities occurred. The charge attained per N atom is $2.71e$ which is less than for the above system ($2.81e$). This charge re-distribution around N-atoms can clearly be seen from the charge density plot in Figure 5. From the band structure calculations, we observed an indirect band-gap opening of 0.48 eV. The value of this energy gap is higher than the calculated value (0.23 eV) of band-gap for the system described in pattern I of the same concentration. The band-gap opening increased because of the unbalancing of two sub-lattices positions due to holes (Be) and electrons (N) doping on different sub-lattices locations.

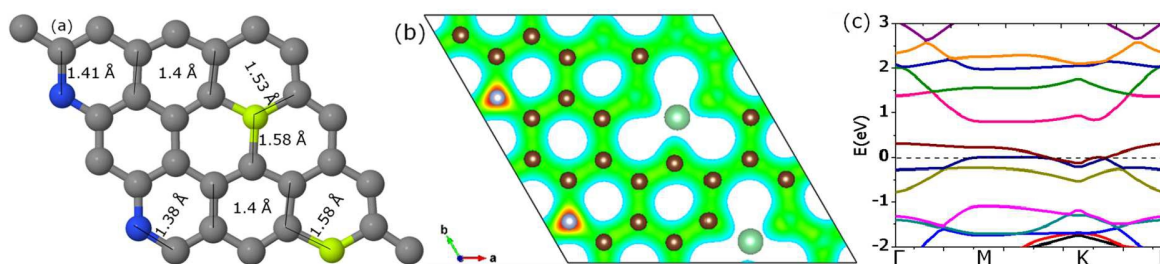


Figure 5: The optimized geometry of graphene sheet co-doped with 2Be and 2N atoms (pattern II) is shown in part (a). Charge density plot can be seen in part (b). The band structure of this optimized geometry is depicted in (c).

3.1.6 Two Be, three N (pattern I)

The impurity concentration in graphene sheet is further enhanced to 15.625 % by replacing five C-atoms with two Be and three N atoms. In the present configuration (pattern-I) the 2 Be and 2 N atoms are replaced with the C-atoms at hexagonal position while 5th C-position is replaced by a N-atom lying at the crossing point of the diagonal making the parallelogram by the four foreign atoms as shown in the part (a) of Fig. 6. As usual Be-C bonds get longer as compared to C-C (1.42) bond distances. The said Be-C bonds are extended either to 1.54 or 1.57 Å. Simultaneously, the C-N bond either remain unchanged or

are slightly shortened to 1.38 Å. The geometrical changes are also reflected in normal C-C bonds as depicted in the Fig. 6(a).

We found the cohesive energy to be -8.14 eV/atom, adequately less than calculated for the previous discussed system and greater than the system doped with two Be and three B (-8.07 eV/atom²⁶). It shows that co-doping of Be with N results in more structural stability than co-doping of Be with B. For the sake of charge transfer information, we made use of Bader analysis, which reveals that Be atoms have lost all their valence charge while C atoms have shifted 4.50e charge to N atoms. The charge transferred per C atom is 0.17e. The average charge assigned per N atom is 2.83e which is greater than for the above case. This local charge density in the proximity of N atoms is shown in Figure 6 (b). The band structure calculations reveal that valence and conduction bands almost touch at Dirac point leaving the system metallic. It is due to the fact that we are injecting holes (Be) and electrons (N) at same sub-lattices sites in graphene sheet.

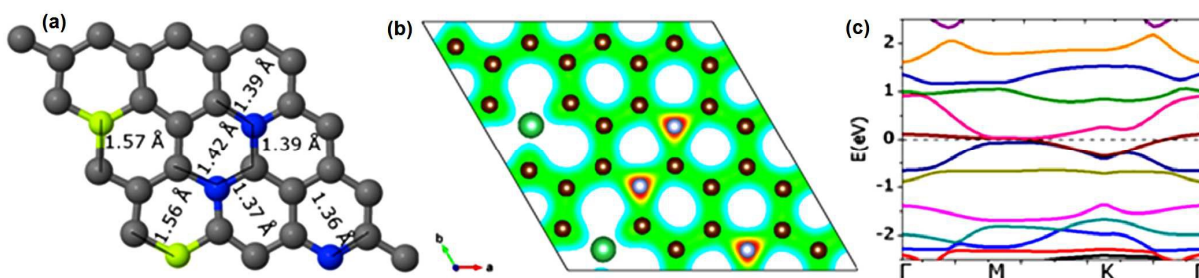


Figure 6: The optimized geometry of graphene sheet co-doped with 2Be and 3N atom (pattern I) is shown in part (a). Charge density plot can be seen in part (b). The band structure of this optimized geometry is depicted in (c).

3.1.7 Two Be, three N (pattern II)

In pattern II of the 15.6% foreign concentration, the replaced Be and N-atoms are heterogeneously incorporated. The geometry optimization results in geometrical variation among the inter-atomic bonds which are shown in part (a) of Fig. 7. As usual Be-C bonds get longer as compared to C-C (1.42) bond distances. The said Be-C bonds are extended either to 1.54 or 1.57 Å. Simultaneously, the C-N bond either remain unchanged or are slightly shortened to 1.38 Å. The geometrical changes are also reflected in normal C-C bonds as depicted in the Fig. 7(a).

Bader charge analysis revealed significant charge redistribution among the system atoms. Be atoms lose all their valence charge lying in their $2s^2$ orbital to the surrounding

atoms Where a variation at large scale (2.41e to 4.47e) is observed (in normal configuration, C has 4 valance electrons, $2s^2, 2p^2$). The main beneficiary of the charge is the N-atoms having average charge of 7.80e relative to the normal valance charge of 5e. This charge depletion near the Be-atoms and higher charge density around the N-atoms can be seen in the charge density plot in Fig. 7(b). This pattern of doping causes slight increase in the energy gap relative to the previous pattern-I. The value of band gap observed is 0.13 eV. The increase in band gap for the same concentration is attributed to impurity injection at hetero sites. The movement of the 3rd N-atom in between the two N-atoms causes to increase the band gap value if compared to the pattern I of this concentration. If we omit the said atom, we are left with Two Be, two N (pattern II) described in section 3.1.5 configuration where significantly higher band-gap was achieved. The nature of the energy-gap is indirect one here. The band-gap lies slightly above the Fermi level. No Dirac cone is observed. The system emerges as a result of simultaneous insertion of holes (Be) and electrons (N).

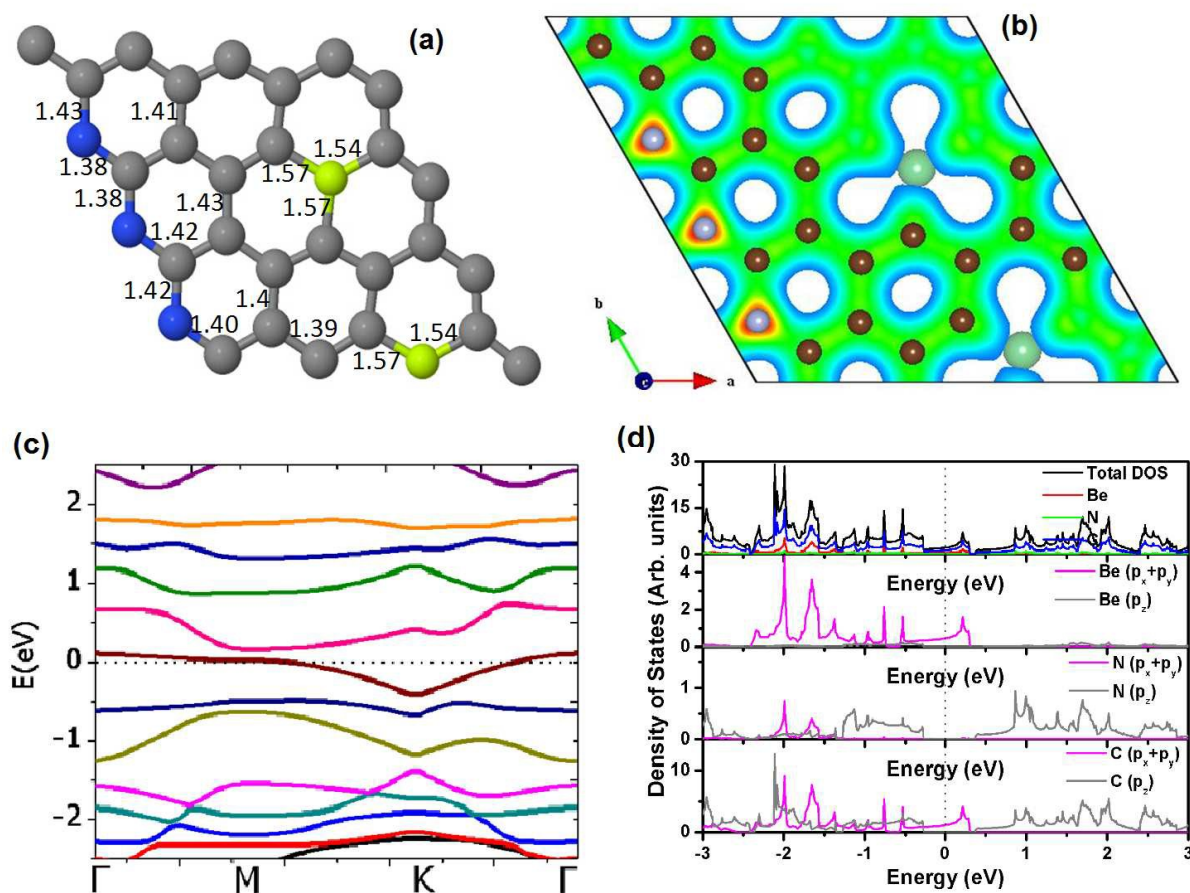


Figure 7: The optimized geometry of graphene sheet co-doped with 2Be and 3N atom (pattern II) is shown in part (a). Charge density plot can be seen in part (b). The band

structure of this optimized geometry is depicted in (c). TDOS and PDOS graphs are drawn in (d).

The total density of states (DOS) and the projected density of states (PDOS) calculations were performed in order to further investigate the role of dopants. The results are presented in Fig. 7(d) which indicate that the Be atom's hybridized $P_{x/y}$ orbitals (formed by sp^2 hybridization of the $2s$, $2p_x$ and $2p_y$ orbitals) strongly interact with the sp^2 hybridized $p_{x/y}$ orbitals of carbon atoms. This interaction exists at a wide energy range. The p_z orbital of C also significantly contributes to the DOS by providing itinerancy to the electrons in the graphene sheet. Whereas Be's p_z orbital has negligibly small contribution in valance as well as conduction band. The population at the Fermi level also comes from the $2p_{(x+y)}$ orbitals of Be and C where infinitesimally small DOS is coming from x and y orbital of N. This strong overlapping between these p orbitals results in σ bonds formation over an energy range from -2.35 eV to 0.35 eV (approx.). The p_z orbitals of carbon and nitrogen overlap in conduction band resulting in π bond formation in a wide energy range. Entire DOS population in the conduction band is contributed in decreasing order by C, N and Be. Lastly, the DOS from the P_z orbitals of all the three elements contribute over the reported energy range except at around the Fermi level.

3.1.8 Two Be, three N (pattern III)

Since we are interested in having a comprehensive study regarding the effect of doping site on the band-gap, thus another change in the structure relative to pattern II with the same composition was done. In the present pattern one of the N-atoms was moved to form a new configuration as depicted in Fig. 8 (a). In the new configuration geometrical changes occur as a result of geometry optimization. However, these changes are not much different from as observed in pattern II and can be seen in the above referred figure. As usual Be atoms have lost all valence electrons to C and N-atoms. Resulting charge redistribution on the C-atoms has been found to be ranging from $1.75e$ to $4.54e$ while N-atoms have gained a significant accumulation of charge (7.71 to $7.85e$). The radish area around the N-atoms shows the higher concentration of charge in charge density plot shown in Fig. 8 (b). The configuration under discussion bears higher value (0.35 eV) of band-gap relative to the previous doping pattern where energy gap was 0.13 eV. However, nature and position of the band-gap is unaltered. These changes in band-gap value due to variation in dopant site allow us to conclude that having control on the doping position(s), facilitates one to tune the energy gap minutely to some desired level.

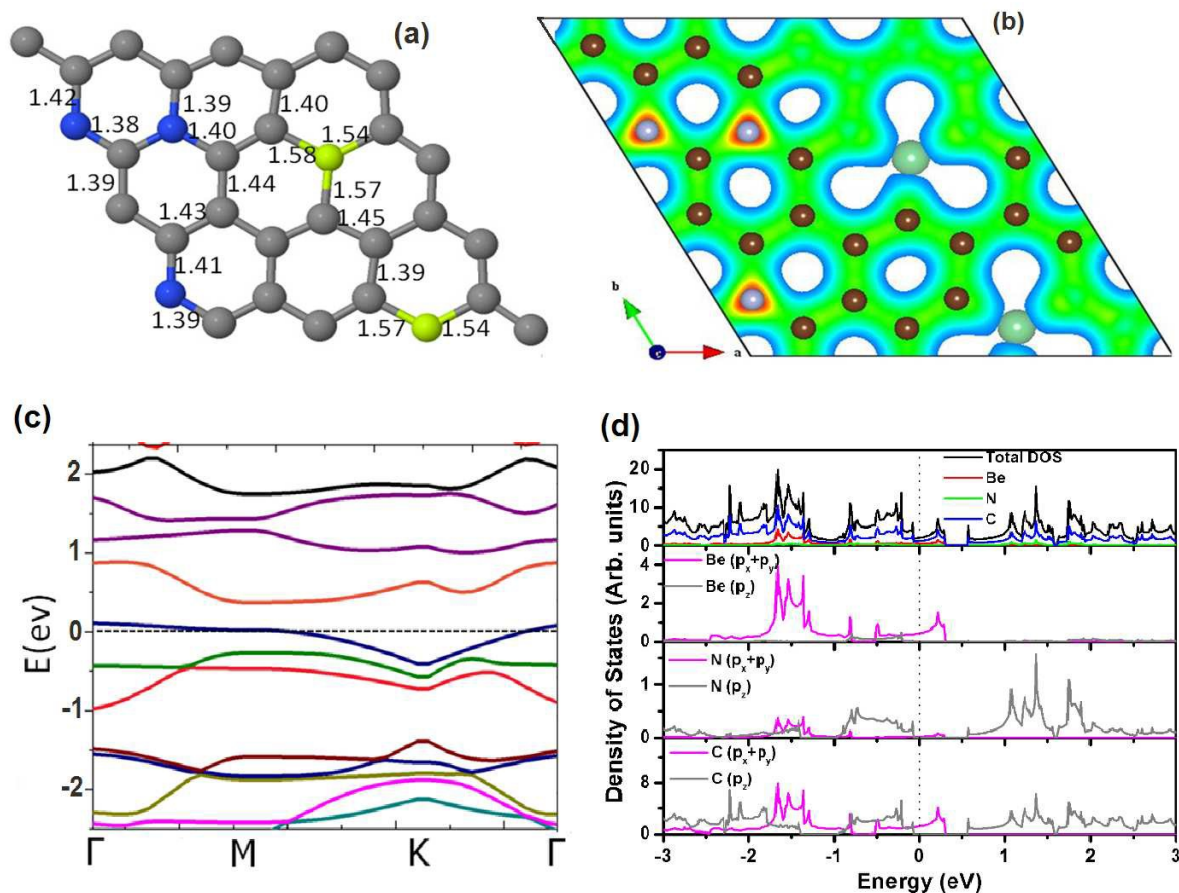


Figure 8: The optimized geometry of graphene sheet co-doped with 2Be and 3N atom (pattern III) is shown in part (a). Charge density plot can be seen in part (b). The band structure of this optimized geometry is depicted in (c). TDOS and PDOS graphs are drawn in (d).

The DOS and the PDOS calculations were performed for further investigations. The results are presented in Fig. 8(d). It is clear that sp^2 hybridized $p_{x/y}$ orbitals of Be strongly interact with the hybridized $p_{x/y}$ orbitals of carbon atoms. Again the contribution from the N-atoms is very limited. The interaction is very strong in the energy range -1.5 to -2.0 eV. Additionally, in this energy range $p_{x/y}$ orbitals of N (although negligible) also network relatively more prominently as compared to the previous patterns thus contributing in sigma bonds formation. Hence, some area all around the Fermi energy is observed populated due to the σ bonding from $p_{x/y}$ orbitals of C and Be and a minute contribution from N $p_{x/y}$ orbitals. This means that at the Fermi level only sigma bonds are formed. The p_z orbital of all the three elements contribute in all the reported energy range except at energy gap. Nonetheless, the prominent portion is coming from the C with somewhat significant contribution from N and the lowest input by Be atoms. It's important to note that substantial intensity of DOS

from these three elements' p_z orbitals is found in hybridization (of low intensity) either just below to -1.0 eV energy range or above the band gap (of higher intensity). The contribution of DOS decreases in order as C, N and Be. Thus the π bond formation is found just below the Fermi level or above the energy-gap (more significant) as a result of p_z orbitals overlapping majorly from C and N.

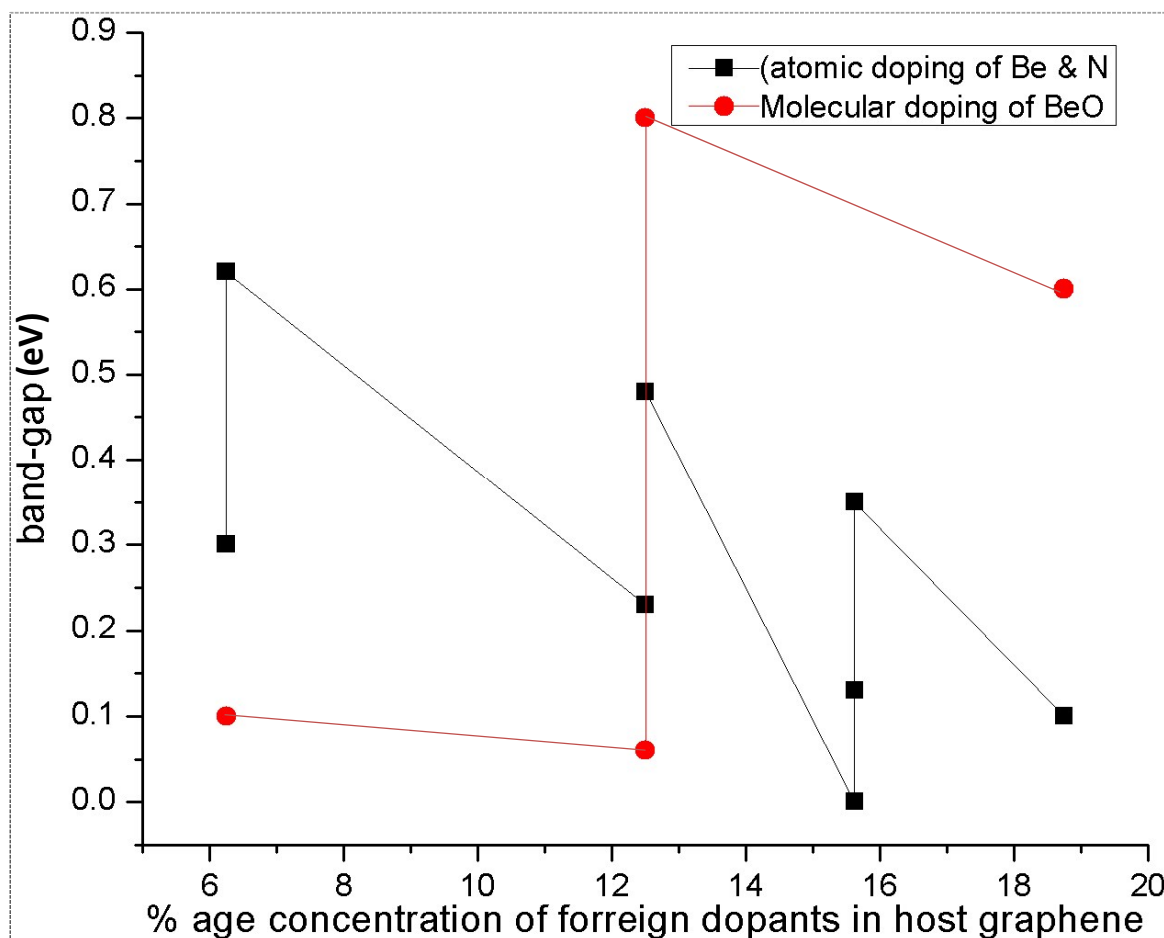
Another arrangement calculated is by changing the position of the left most N-atom (in Fig. 8a) displaced on the right towards its neighbor N in top row. But the value of band-gap remained about 0.10 eV.

Table 2: Summary of the results obtained for Be and N co-doping and BeO molecular doping in graphene.

Dopants types	Concentration (%)	Pattern	Cohesive energy (eV/atom)	Band-gap (eV)
1Be, 1N	6.25	Same sub-lattice sites (pattern I)	-8.73	0.30
1Be, 1N	6.25	Different sub-lattice sites (pattern II)	-8.73	0.62
2Be, 2N	12.5	Same sub-lattice sites (pattern I)	-8.27	0.23
2Be, 2N	12.5	Different sub-lattice sites (pattern II)	-8.28	0.48
2Be, 3N	15.625	Same sub-lattice sites (pattern I)	-8.14	0.0
2Be, 3N	15.625	Change Be & N (pattern II)	-8.14	0.13
2Be, 3N	15.625	Change 1 N (pattern III)	-8.15	0.35
1BeO	6.25		-8.61	0.10
2BeO	12.5	Pattern I	-8.00	0.06
2BeO	12.5	Pattern II	-8.00	0.80

3BeO	18.75	Pattern I	-7.39	0.60
3BeO	18.75	Pattern II	-7.37	0.82

Four different systems with varying dopant site for N-atom were investigated to tune the Band-gap. The effect of co-doping of Be and N is found dissimilar to that of co-doping of Be and B. In case of co-doping of Be and B, when heterogeneous species are integrated at same sub-lattice positions, the resultant band-gap has a maximum value. However, to achieve a larger value of band-gap with co-doping of Be and N, both the impurities should be incorporated at different sub-lattice sites. This effect can be understood that Be and B both act as hole doping while N act as electron doping in graphene. More-over, by increasing doping concentration beyond 6.25 %, the band-gap changes to a lesser value.



Graph 1: Graph explicitly explains the vital role of dopant position of foreign elements. For the same concentration but variable dopant position leads to significant different value of band gap.

3.2 Molecular doping

After atomic doping, we turned to a molecular doping of BeO. In this section we have discussed the doping of 1BeO, 2BeO, and 3BeO molecules in graphene sheet. The change in the band-gap with site variation has also been explored and reported.

3.2.1 1BeO molecule

Initially, we doped single molecule of BeO with Be-O axis parallel to the graphene sheet which makes the impurity concentration of 6.25 % in the system. After structural minimization, the changes in geometrical structure of graphene occurred. The Be-O bond length was increased from 1.34 Å (as found in gas phase computation) to 1.5 Å. The Be-C bonds around Be were elongated up to 1.56 Å as shown in Figure 9 (a). Consequently, next neighboring C-C bond lengths were altered, minimum value being 1.39 Å. However, the C-O bond length (1.42 Å) is same as C-C bonds in clean pristine graphene. Cohesive energy is found to be -8.61 eV/atom, which is lower than co-doping of Be with B or N. But it is more stable than if two Be-atoms are doped (-8.49 eV/atom). O atom being more electronegative compared to Be and C atoms, has gained 1.60e as a result of 2e valence charge lost by Be-atom. Net charge given by BeO molecule to graphene is 0.403e. Consequently, charge redistribution on C atoms ranges from 3.68e to 4.56e. The average charge gain per C atom is 0.013e. A significant amount of the charge shifted from Be is sucked by O-atom as depicted in iso-surface plot of the charge density (see Figure 9 (b)). In the co-doping of Be and N, the N specie sucks the charge from Be as well as C atoms, but in this case some portion of the charge that shifted from Be atom is taken by C-atoms. The electronic structure of the system is calculated which shows a small band-gap opening of 0.10 eV. Band-gap was shifted from K, and found to be somewhere in the middle of K and M points. As electrons and holes are being injected in the system simultaneously, thus no shift in Fermi level is observed. Hence, the band-gap is proficient than the above systems.

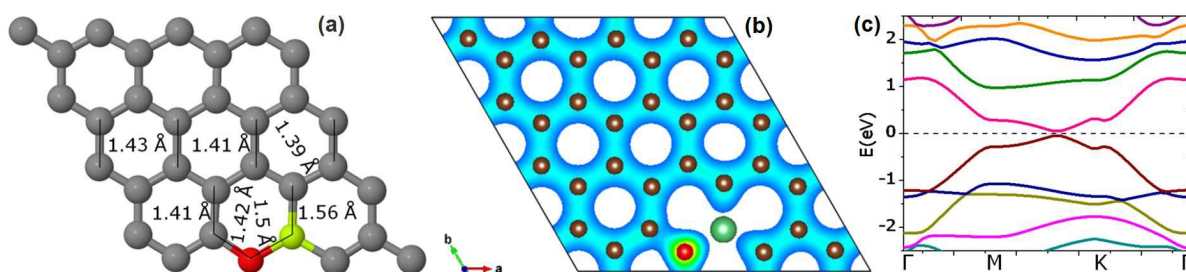


Figure 9: The optimized geometry of graphene sheet doped with one BeO molecule is shown in part (a) where green and red spheres represents Be and O atoms respectively. Charge density plot can be seen in part (b). The band structure of this optimized geometry is depicted in (c).

3.2.2 Two BeO molecules (pattern I)

Replacement of 4 C-atoms by 2 BeO molecules in graphene leads the doping concentration to be 12.5 %. Different sub-lattice sites chosen for BeO molecules are depicted in Figure 10(a). After geometry optimization, some inter-atomic bonds were stretched while others were compressed. The geometrical changes were quite similar as discussed previously in case of single BeO molecule doping. The cohesive energy is decreased to a value of -8.00 eV/atom. This value is adequately lower than that of observed for co-doping of two Be and two N doping (-8.27 eV/atom). As usual Be transfers complete valence charge to C and O-atoms. The major portion of this charge accumulates around O atoms (see Figure 10(b)). The O-atoms have attained a charge of $3.18e$ which means that $1.60e$ charge per O atom is gained. The charge transferred per BeO molecule to C atoms is $0.822e$. Hence, new value of charge is assigned to C atoms (ranging from 3.63 to $4.54e$) average gain being $0.03e$ per C atom. We calculated the electronic structure for this system (see Figure 10 (c)). This time band-gap opening was observed on K high symmetry point with a small value of 0.06 eV. The BeO molecules were embedded at different sub-lattice positions, which resulted into the reduction of the band-gap. The impurity atoms bear electropositive and electronegative character relative to graphene, the Fermi level remains at zero level.

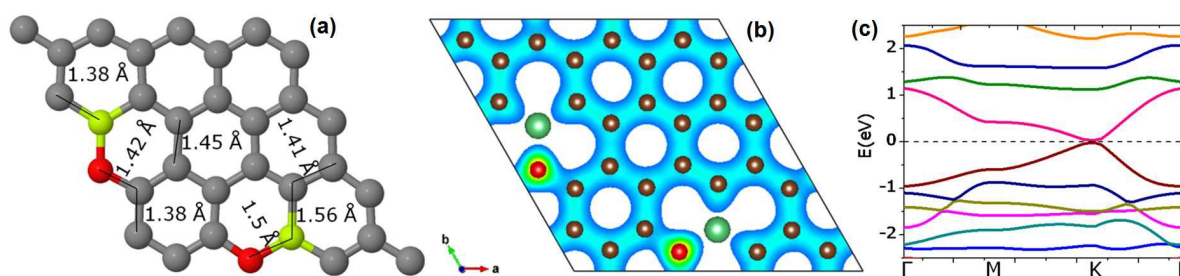


Figure 10: The optimized geometry of graphene sheet doped with 2BeO molecule (pattern I) is shown in part (a) (as mentioned in previous figure, green and red spheres represents Be and O atoms respectively). Charge density plot can be seen in part (b). The band structure of this optimized geometry is depicted in (c).

3.2.3 Two BeO (pattern II)

In this new configuration, same (type and number) impurities as in above case are mingled in graphene sheet but in this new configuration both BeO molecules reside on same sub-lattice sites. After structure relaxation process, the Be-C bonds were equally stretched to 1.54 Å. The bonds in the proximity of O were 1.42 Å, same as C-C distance in graphene. The Be-O distances are also observed to be same (1.5 Å) as found in above case as shown in Figure 11 (a). Additionally, no change in cohesive energy of the system is found relative to above model. Similarly, the charge redistribution among the various atoms of the model resulting from the doping of 2 BeO molecules at these positions is same as above case. The only difference found is the range (from 3.51 to 5.36e) of charge on C atoms. In contrast to the facts that changes in geometrical parameters, stability of the structure and charge redistribution is not realized differently relative to the model investigated in pattern I, the magnitude of band-gap is drastically enhanced. We observed an indirect band-gap of 0.80 eV. An enormous increase in band-gap of 0.74 eV occurred just by changing the dopants site. It is because that on one sub-lattice sites we are injecting holes (Be) and on other sub-lattice sites, electrons (O) are infused.

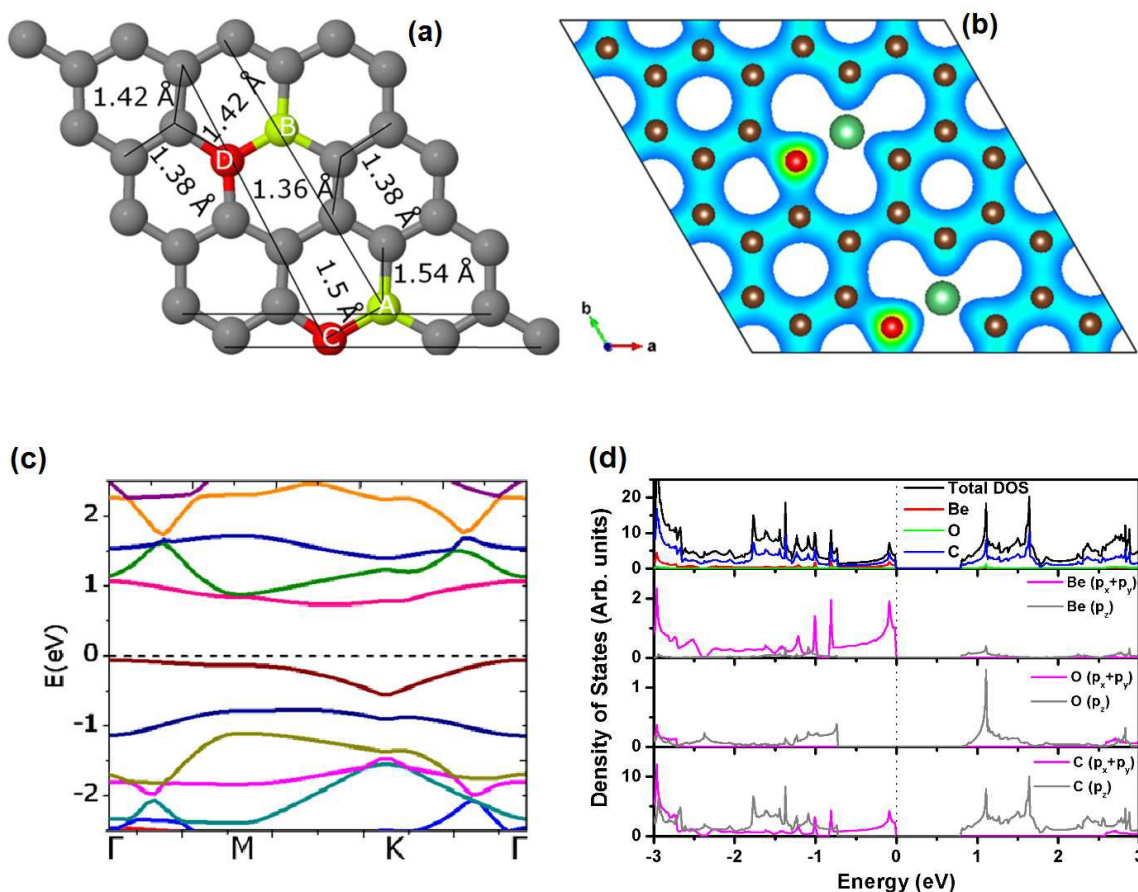


Figure 11: The optimized geometry of graphene sheet doped with 2BeO molecule (pattern II); with green and red spheres depicting Be and O atoms respectively; is shown in part (a). Charge density plot can be seen in part (b). The band structure of this optimized geometry is depicted in (c). TDOS and PDOS are drawn in (d).

Figure 11 (d) reflects that among $2p_{x/y}$ orbitals from C and Be atoms, strong hybridization exists in the valence band region resulting in sigma bond formation. A small mixing of $2p_{x/y}$ orbital of O atoms is observed below -2.6 eV and above $+2.6$ eV in a small energy range (0.4 eV). The contribution from the O remains missing almost in the whole energy range reported except lower intensity overlapping between Be and O $2P_{x/y}$ orbitals near the end of the conduction band is seen. DOS from p_z orbitals by all the three elements is found in the whole reported energy range but disappears 0.8 eV (approx.) below and above the Fermi level. However, the contribution decreases in order C, O and Be. Thus π bond formation both in valance and conduction band is mainly resulting from overlapping of C and O p_z orbitals. The important difference between the previous and present discussions

regarding PDOS is the overlapping of p_{xy} orbitals of O and C near the end of conduction band.

3.2.4 Three BeO molecules (pattern I)

We increased the foreign dopant concentration percentage to 18.75% in graphene sheet by replacing three BeO molecules such that two BeO molecules reside on same sub-lattice positions while the third BeO molecule is assigned to different sub-lattice sites. Geometry optimization was performed until a fully relaxed structure was achieved. The Be-C bond lengths were stretched to different values (ranging from 1.51 to 1.55 Å). The C-O bonds were in the range from 1.38 to 1.44 Å as shown in Figure 12 (a). Simultaneously, Be-O bond lengths are elongated up to 1.5 Å. The structure stability was reduced as the cohesive energy is reduced to -7.39 eV/atom, adequately lower than the system discussed above (-8.00 eV/atom). The charge density around O atoms increased as Be atoms have shifted their total valence charge. The charge retained by O atoms is $4.87e$ ($1.62e$ per O atom), which is greater than the charge gain of $1.59e$ per O atom for the previous case. The charge transfer to graphene sheet is calculated to be $1.13e$ per BeO molecule causing the charge redistribution on C atoms from 2.80 to $4.74e$. The average charge gain per C atom is $0.043e$. Although the nature (indirect) of the band-gap was observed to be the same as above mentioned case but its magnitude was reduced to 0.60 eV relative to 0.80 eV obtained in case of two BeO molecules positioned at hetero sites. However, this value is significantly higher compared to 1BeO doping. This reduction in band-gap is due to the particular location of BeO molecules in graphene sheet.

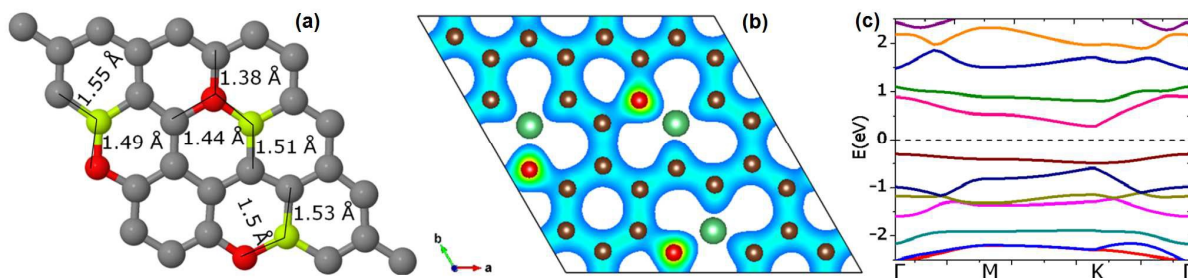


Figure 12: The optimized geometry of graphene sheet doped with 3BeO molecules (pattern I) is shown in part (a). Charge density plot can be seen in part (b). The band structure of this optimized geometry is depicted in (c).

3.2.5 Three BeO molecules (Pattern II)

This pattern of 3 BeO molecules shows that how the site variation in replacement causes a band-gap to change both in magnitude and position. Here relative to the previous configuration, 2 BeO molecules have changed their positions while third lies at the same location as can be seen in Fig. 13(a). The local geometrical changes are not much different relative to previous cases. As usual the longest bond distances are between Be and C, lower ones are between Be and O and, the smallest ones are those where O atoms are associated with C atoms or C-C bonds. All these changes occurred are visible in Fig. 13(a). The charge density plot depicted in Fig. 13(b) shows reddish spots near the O atoms. This charge accumulation is due to the extra charge received from Be atoms which lose their entire valance ($2 \times 3 = 6e$) electrons (see charge depletion around Be in Fig. 13(b)). The $4.9e$ charge is received by O atoms (being more electronegative) while remaining $1.1e$ are distributed in the graphene sheet where charge variation occurs from 2.83 to $5.44e$ as dictated by Bader charge analysis.

The electronic structure calculations reveal a band-gap of 0.82 eV. The energy gap is found in the conduction band starting almost from the Fermi energy. In agreement with the previous configuration, the nature of the band-gap is indirect; nevertheless, the magnitude is substantially enhanced. The band gap is almost similar in magnitude and nature with the configuration described in case of 2Be molecules doping at hexagonal positions (section 3.2.3). Its important to note that concentration of 18.75% when doping sites are not symmetric, produces a similar band-gap as of 12.5% symmetric doping concentration. This observation clearly indicates that the doping site is of critical importance for creation of band-gap in agreement with a recent observation.⁴³ No Dirac cone is observed and linear dispersion is destroyed.

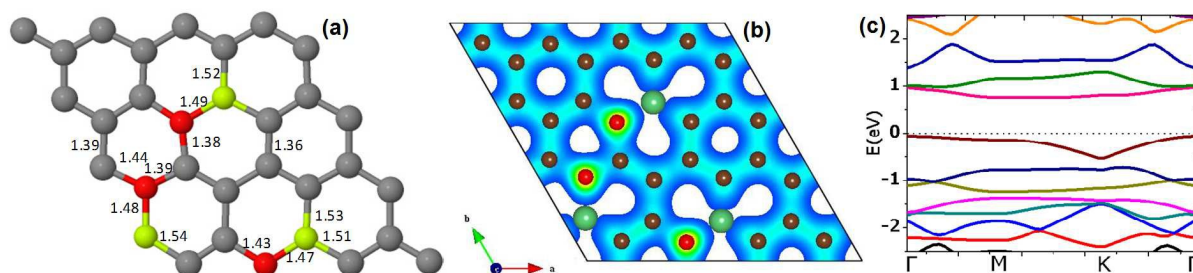


Figure 13: The optimized geometry of graphene sheet doped with 3BeO molecule (pattern II) is shown in part (a). Charge density plot can be seen in part (b). The band structure of this optimized geometry is depicted in (c).

4 Conclusions

The structural and electronic properties of beryllium (Be) and nitrogen (N) co-doped and BeO molecular doped graphene systems were investigated employing density functional theory (DFT) calculations. The central focus was on how the band-gap can finely be tuned as a function of concentration and replacement site(s) change. As a general conclusion the bond lengths around Be atom(s) expand while bond shrink around N atom(s) relative to the clean graphene system in the optimized structures. The O atom(s) render the structure almost unaltered. The Fermi level rises or lowers depending upon the doped concentration of hole(s) or electron(s). Simultaneous doping of a hole (1Be) and electron (1N) produces a small energy-gap of 0.30 eV, which is lower than the case when only 1 Be atom is doped.²⁶ The gap opening increases in the case when Be and N are substituted on the same hexagon. The impurity substitution integrated at different sub-lattice positions cause to enhance the band-gap to 0.62 eV. If holes and electrons are substituted at the same sub-lattice positions (A or B sites) then band-gap is reduced. The foreign dopant concentration always does not help to enhance the band-gap but even reduction in energy-gap may occur on concentration increase subject to site variation. Additionally, the insertion of BeO molecule(s) is also position dependent and energy-gap is not always proportional to the density of doped BeO molecules. Hence, choosing a combination of sites for doping is of vital importance. Finally, our results suggest that having control on the dopant position, a very fine tuning of the band-gap is possible which make graphene a favorable material for its utilization in diverse electronic device applications.

Reference List

1. A. K. Geim and K. S. Novoselov, *Nat Mater*, 2007, **6**, 183.
2. P. R. Wallace, *Physical Review*, 1947, **71**, 622.
3. R.Saito, G.Dresselhaus, and M.S.Dresselhaus, *Imperial College Press, London, UK*, 1998.
4. A. H. Castro Neto, F. Guinea, N. M. R. Peres, K. S. Novoselov, and A. K. Geim, *Reviews of Modern Physics*, 2009, **81**, 109.
5. K. S. Novoselov, D. Jiang, F. Schedin, T. J. Booth, V. V. Khotkevich, S. V. Morozov, and A. K. Geim, *Proceedings of the National Academy of Sciences of the United States of America*, 2005, **102**, 10451.
6. Y. Zhang, Y. W. Tan, H. L. Stormer, and P. Kim, *Nature*, 2005, **438**, 201.
7. Y. W. Son, M. L. Cohen, and S. G. Louie, *Nature*, 2006, **444**, 347.
8. T. O. Wehling, K. S. Novoselov, S. V. Morozov, E. E. Vdovin, M. I. Katsnelson, A. K. Geim, and A. I. Lichtenstein, *Nano Letters*, 2008, **8**, 173.
9. K. S. Novoselov, A. K. Geim, S. V. Morozov, D. Jiang, Y. Zhang, S. V. Dubonos, I. V. Grigorieva, and A. A. Firsov, *Science*, 2004, **306**, 666.
10. F. Schedin, A. K. Geim, S. V. Morozov, E. W. Hill, P. Blake, M. I. Katsnelson, and K. S. Novoselov, *Nat Mater*, 2007, **6**, 652.
11. K. S. Novoselov, Z. Jiang, Y. Zhang, S. V. Morozov, H. L. Stormer, U. Zeitler, J. C. Maan, G. S. Boebinger, P. Kim, and A. K. Geim, *Science*, 2007, **315**, 1379.
12. P. Avouris, Z. Chen, and V. Perebeinos, *Nat Nano*, 2007, **2**, 605.
13. K. S. Novoselov, A. K. Geim, S. V. Morozov, D. Jiang, M. I. Katsnelson, I. V. Grigorieva, S. V. Dubonos, and A. A. Firsov, *Nature*, 2005, **438**, 197.
14. A. K. Geim, *Science*, 2009, **324**, 1530.
15. E. V. Castro, H. Ochoa, M. I. Katsnelson, R. V. Gorbachev, D. C. Elias, K. S. Novoselov, A. K. Geim, and F. Guinea, *Physical Review Letters*, 2010, **105**, 266601.
16. R.Lv and M.Terrones, *Materials Letters*, 2012, **78**, 209.
17. F. Schwierz, *Nat Nano*, 2010, **5**, 487.
18. K. Novoselov, *Nat Mater*, 2007, **6**, 720.
19. Xiaolin L, Xinran Wang, Li Zhang, Sangwon Lee, and Hongjie Da, *Science*, 2008, **319**, 1229.
20. M. Y. Han, B. +üzylmaz, Y. Zhang, and P. Kim, *Physical Review Letters*, 2007, **98**, 206805.
21. L. A. Ponomarenko, F. Schedin, M. I. Katsnelson, R. Yang, E. W. Hill, K. S. Novoselov, and A. K. Geim, *Science*, 2008, **320**, 356.
22. B. Trauzettel, D. V. Bulaev, D. Loss, and G. Burkard, *Nat Phys*, 2007, **3**, 192.

23. J. Bai, X. Zhong, S. Jiang, Y. Huang, and X. Duan, *Nat Nano*, 2010, **5**, 190.
24. L. Zhao, R. He, K. T. Rim, T. Schiros, K. S. Kim, H. Zhou, C. Gutiérrez, S. P. Chockalingam, C. J. Arguello, L. Píloví, D. Nordlund, M. S. Hybertsen, D. R. Reichman, T. F. Heinz, P. Kim, A. Pinczuk, G. W. Flynn, and A. N. Pasupathy, *Science*, 2011, **333**, 999.
25. W. J. Yu, L. Liao, S. H. Chae, Y. H. Lee, and X. Duan, *Nano Letters*, 2011, **11**, 4759.
26. S. Ullah, A. Hussain, W. Syed, M. A. Saqlain, I. Ahmad, O. Leenaerts, and A. Karim, *RSC Advances*, 2015, **5**, 55762.
27. P. A. Denis, *Chemical Physics Letters*, 2010, **492**, 251.
28. Aurélien Lherbier, X. Blase, Yann-Michel Niquet, François Triozon, and Stephan Roche, *Physical Review Letters*, 2008, **101**, 036808.
29. M. Wu, C. Cao, and Z. J. Jiang, *Nanotechnology*, 2010, **21**, 505202.
30. O. Leenaerts, B. Partoens, and F. M. Peeters, *Phys. Rev. B*, 2008, **77**, 125416.
31. Pinto H, Jones R, Goss JP, and Briddon PR, *J Phys Condens Matter*, 2009, **21**, 402001.
32. P. A. Denis and C. Pereyra Huelmo, *Carbon*, 2015, **87**, 106.
33. P. A. Denis, C. P. Huelmo, and F. Iribarne, *Computational and Theoretical Chemistry*, 2014, **1049**, 13.
34. L. S. Panchakarla, S. K. Saha, S. K. Saha, .Govindaraj, H. R. Krishnamurthy, . V. Waghmare, and N. R. Rao, *Advanced Materials*, 2009, **21**, 4726.
35. Wei D, Liu Y, Wang Y, Zhang H, Huang L, and Yu G, *Nano Letters*, 2009, **9**, 1752.
36. Y. Fan, M. Zhao, Z. Wang, and H. Zhang, *Appl. Phys. Lett.*, 2011, **98**, 83103.
37. X. Fan, Z. Shen, A. Q. Liu, and J. L. Kuo, *Nanoscale*, 2012, **4**, 2157.
38. A. K. Manna and S. K. Pati, *The Journal of Physical Chemistry C*, 2011, **115**, 10842.
39. D. H. Wu, Y. F. Li, and Z. Zhou, *Theoretical Chemistry Accounts*, 2011, **130**, 209.
40. J. Zhu, M. Chen, Q. He, L. Shao, S. Wei, and G. Guo, *RSC Advances*, 2013, **3**, 22790.
41. Y. H. Zhang, L. F. Han, Y. H. Xiao, D. Z. Jia, Z. H. Guo, and F. Li, *Computational Materials Science*, 2013, **69**, 222.
42. Y. Ferro, A. Allouche, and C. Linsmeier, *J. Appl. Phys.*, 2013, **113**, 213514.
43. Pooja Rani and V. K. Jindal, *Applied Nanoscience*, 2014, **4**, 989.
44. P. Rani and V. K. Jindal, *RSC Advances*, 2013, **3**, 802.
45. G. Kresse and J. Furthmüller, *Physical Review B*, 1991, **44**, 13298.
46. G. Kresse and J. Hafner, *Physical Review B*, 1993, **47**, 558.
47. P. E. Blochl, *Physical Review B*, 1994, **50**, 17953.
48. J. P. Perdew, K. Burke, and M. Ernzerhof, *Physical Review Letters*, 1996, **77**, 3865.

49. H. J. Monkhorst and J. D. Pack, *Physical Review B*, 1976, **13**, 5188.
50. M. Methfessel and A. T. Paxton, *Physical Review B*, 1989, **40**, 3616.
51. P. Pulay, *Chemical Physics Letters*, 1980, **73**, 393.

